SATELLITE CLUSTER FLIGHT DESIGN CONSIDERATIONS

Jason Schmidt(1), Mike Phillips(2), and Matthew Ruschmann(3)
(1)*Emergent Space Technologies, 355 S Teller St Ste 200, Lakewood, CO 80226, 720-837-2464, jason.schmidt@emergentspace.com*
(2)*Emergent Space Technologies, 355 S Teller St Ste 200, Lakewood, CO 80226*
(3)*Emergent Space Technologies, 6411 Ivy Lane Ste 303, Greenbelt, MD 20770*

Keywords: *Proximity Operations, Relative Motion, Cluster Flight, Formation Flying*

Abstract: *The challenges of designing optimal satellite cluster configurations are presented with respect to several key considerations including passive safety, stability, packing ratio, minimization of the inter-module cone angles, scalability, and observability with relative range measurements. A short primer on relative orbit elements (ROEs) and relative satellite motion precedes a discussion of these metrics. ROE and safety ellipse concepts can be used to intuitively construct several different cluster geometries that optimize different constraints such as packing ratio, stability, or inter-module cone angles. Unique contributions from the authors include cluster stability in terms of ROEs, optimizing the packing ratio while maintaining passive safety, radial, intrack, crosstrack (RIC) and inertial intermodule cone angles for passively safe trajectories, relative state observability using intermodule range measurements in four module clusters, and the pros and cons of three general configurations known as Nested, Circles-in-Circles, and Cross configurations.*

1. Introduction

Safe and efficient long duration cluster flight is a necessary capability in order to enable autonomous, cooperative interaction between satellites in a cluster. Interest in clusters is evident with missions like the European Space Agency's PRISMA mission [8] and mission concepts such as DARPA's System F6 [2], which was conceived to demonstrate long duration cluster flight by demoing a four satellite cluster on a six month mission. Several considerations must be taken into account when attempting long duration cluster flight, among which are fuel usage, probability of collision between modules, intermodule communication, navigation observability, as well as mission objectives. These various considerations are often competing. For a given mission these considerations must be weighed when selecting a cluster geometry, so that the mission objectives can be met.

This paper discusses several considerations key to designing useful cluster geometries, and leverages the intuitive relative orbit element (ROE) representation of relative orbital motion to aid the discussion. Related publications for passive safety, stability, packing ratio, and observability are noted in the relevant section. Unique contributions from the authors include cluster stability in terms of ROEs, optimizing the packing ratio while maintaining passive safety, radial, intrack, crosstrack (RIC) and inertial intermodule cone angles for passively safe trajectories, and relative state observability using intermodule range measurements in four module clusters. Three passively safe cluster configurations known as Nested, Circles-in-Circles, and Cross are defined and their relative strengths and weakness are discussed. These cluster configurations would be useful starting points for the development of cluster configurations for future cluster flight missions.

2. Relative Orbit Elements Primer

The six elements of the state vector in the radial, intrack, crosstrack (RIC) frame can be transformed into six relative orbit elements (ROE) described by [14, 16, 15]. These elements are obtained by algebraic manipulation of Clohessy-Wiltshire Equations and by realizing that all relative orbits can be represented as traveling ellipses. The relative orbit elements are given by Eq. 1. The in-plane ROEs are shown graphically in Fig. 1.

$$\begin{aligned}
x_d &= 4x + 2\frac{\dot{y}}{\omega} & y_d &= y - 2\frac{\dot{x}}{\omega} \\
a_e &= 2\sqrt{\left(\frac{\dot{x}}{\omega}\right)^2 + \left(3x + 2\frac{\dot{y}}{\omega}\right)^2} & \beta &= \operatorname{atan2}\left(\dot{x}, 3\omega x + 2\dot{y}\right) \\
z_{max} &= \sqrt{\left(\frac{\dot{z}}{\omega}\right)^2 + z^2} & \psi &= \operatorname{atan2}\left(\omega z, \dot{z}\right)
\end{aligned} \tag{1}$$

where ω is the orbital rate, x_d and y_d represent the downrange and radial position of the center of the traveling ellipse, a_e represents the semi-major axis of the traveling ellipse, z_{max} represents the maximum out-of-plane displacement of the ellipse, and β and ψ are the phase angles of the in-plane and out-of-plane sinusoidal motion. The difference between ψ and β is known as γ, and is often useful in characterizing relative orbit element constraints.

$$\gamma = \psi - \beta \tag{2}$$

Equation 1 can be solved to obtain equations for the ROE as a function of time.

$$\begin{aligned}
x_d &= x_{d0} & y_d &= y_{d0} - \tfrac{3}{2}\omega x_{d0} t = y_{d0} - \tfrac{3}{2}\omega x_d t \\
a_e &= a_{e0} & \beta &= \beta_0 + \omega t \\
z_{max} &= z_{max0} & \psi &= \psi_0 + \omega t
\end{aligned} \tag{3}$$

These relative orbital elements can also be used to find the elements of the relative state vector in the RIC frame.

$$\begin{aligned}
x &= \frac{-a_e}{2}\cos\beta + x_d & \dot{x} &= \frac{a_e}{2}\omega\sin\beta \\
y &= a_e \sin\beta + y_d & \dot{y} &= a_e n \cos\beta - \tfrac{3}{2}\omega x_d \\
z &= z_{max}\sin\psi & \dot{z} &= z_{max}\omega\cos\psi
\end{aligned} \tag{4}$$

When mapping inertial states to ROEs, the inertial states are first transformed to RIC coordinates according to [1], and then the RIC coordinates may be transformed to ROEs by Eq. 1. When transforming between the inertial frame and the RIC frame, the curvature of the orbit should be taken into account. As such, y represents the distance downrange from the origin along the curvature of the reference orbit, and z represents the separation along the curved crosstrack. All of the results presented also have an additional correction to the intrack velocity to ensure that the modules maintain the same relative orbital period before and after the transformation is performed.

$$\dot{y} = \frac{\omega}{2}\left(\Delta a - 4x\right) \tag{5}$$

where Δa represents the difference in semi-major axis between the module and the reference orbit.

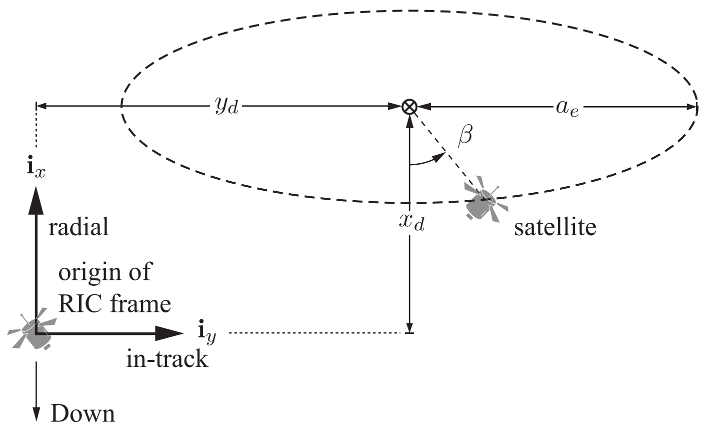

Figure 1: In-plane Relative Orbit Elements (ROEs)

3. Passive Safety

An on-orbit collision is one of the worse fates possible for a cluster mission. In order to avoid the cost and impact of such an event, it is important that clustered modules are arranged in such a way that collisions will not occur even if there is a total loss of control. Relative trajectories that satisfy these conditions are referred to as passively safe trajectories or safety ellipses in [9].

First, it should be noted that crosstrack motion in Eq. 4 is oscillatory, and, even if higher order effects are taken into account, the magnitude and period of the crosstrack motion will change only very slowly according to [17]. Thus, errors in crosstrack positioning will not likely lead to unexpected collisions.

Radial and intrack motion, on the other hand, are tightly coupled with intrack secular drift directly dependent on radial position in Eq. 3. Thus, small errors in semi-major axis will always lead to intrack drift. It is not possible to perfectly insert satellites into their desired orbits and, in addition, satellites experience different forces due to perturbations such as drag and solar radiation pressure.

These differential perturbations cause the semi-major axes of their orbits to differ. This manifests itself in differential drift primarily in the intrack direction (v-bar). Thus, the main factor affecting the passive safety of a configuration is separation between modules in the radial-crosstrack plane (r-bar, h-bar).

Passively safe ROE trajectories with respect to a module at the origin can easily be identified. First, x_d should be nominally zero. If x_d is almost as large as $a_e/2$, then the relative trajectories will not be passively safe. Second, a_e and z_{max} should be significantly larger than the combined hardbody radii of the two modules involved. Finally γ should be close to either 0° or 180°. If γ is close to 90° or 270° the relative trajectories will not be passively safe.

4. Stability

While the initial cluster configuration may be designed to be passively safe, the effect of higher order gravity perturbations on the cluster configuration can distort the original geometry. The goal is to design the cluster configuration in a way that minimizes cluster distortion due to higher-order gravity terms, decreases fuel usage and improves passive cluster safety. Creating a cluster that keeps all of the modules at the same inclination and according to [18, 17] flying the whole cluster at the critical inclination of 63.43° are two ways to mitigate the effect of these perturbations.

Much work, [10, 13], has been done to explore J2-invariant formations. Aside from a difference in semi-major axis between the modules, the next biggest driver of secular drift is a difference in inclination. Ensuring that the sum of β and γ is equal to either 90° or 270° at the ascending node is one way to ensure that the modules are at the same inclination as the origin.

$$\operatorname{mod}(\gamma+\beta, 180^\circ) = 90^\circ \tag{6}$$

A non-zero z_{max} can still be achieved with this constraint, but the crosstrack motion will be due entirely to a difference in right ascension of the ascending node. The four module Nested configuration shown in Fig. 2 and described in Tab. 1 achieves just that. Figure 2 shows both the cluster configuration and the ROE perturbations for a cluster flying at 600 km altitude with 45° inclination. The cluster is propagated for 20 orbits with a 20x20 gravity model and no other perturbations. With this configuration the majority of the ROEs have no noticeable secular drift, and most importantly there is no secular intrack drift. The two ROEs with a significant amount of drift are the phase angles γ and β. If β was propagated using the mean angular rate of the argument of latitude of the reference orbit instead of the osculating angular rate of the true anomaly, then no drift in β would exist, and γ would drift by the rate of precession of the orbit.

As shown in Fig. 3, by flying the configuration at the critical inclination of 63.43° the drift in γ is also eliminated. The drift in β still exists and has the effect of causing β to have a period of less than one orbit, however the relative β between the modules remains constant, and the shape of the cluster is undisturbed.

For cluster formation with modules that are not at the same inclination, often times the fuel consumption between the modules can be balanced by adjusting the initial β angle. For a cluster of four modules shown in Fig. 4 and described in Tab. 2, two of the modules experience different

y_d drift rates than the others. Fuel consumption amongst the modules could be more evenly distributed by setting the β's to 45°, 135°, 225°, and 315°, instead of the 0°, 90°, 180°, and 270° shown. This would have the effect of causing all of the modules to drift from the reference orbit at roughly the same rate, although in different directions.

Atmospheric drag is a significant perturbation at lower altitudes, and clusters with large a_e values would experience differential drag that would tend to pull the cluster apart. Keeping the cluster as small as possible, as discussed in the next section, would help mitigate these effects (assuming the modules have the same ballistic coefficient).

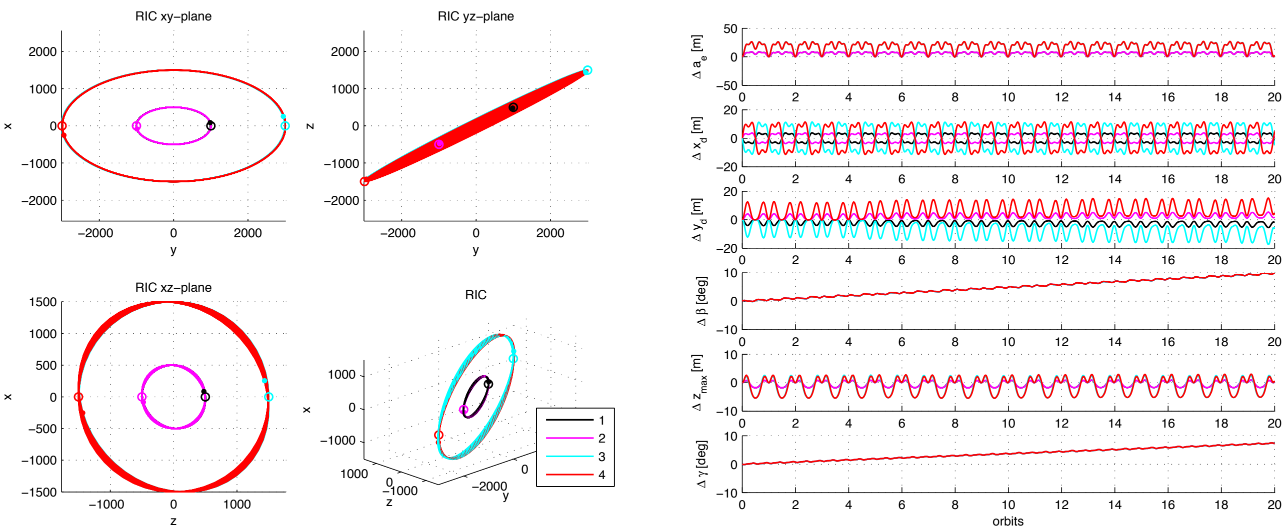

Figure 2: ROE secular drift in β and γ for Nested cluster configuration with 4 modules, propagated for 20 orbits using a 20×20 gravity model. The orbit has an altitude of 600 km and is inclined at 45°.

Table 1: Relative Orbit Elements (ROE) for four module Nested formation in Fig. 2 at the ascending node.

Module	a_e (m)	x_d (m)	y_d (m)	β (degrees)	z_{max} (m)	γ (degrees)
1	1000	0	0	90	500	0
2	1000	0	0	270	500	0
3	3000	0	0	90	1500	0
4	3000	0	0	270	1500	0

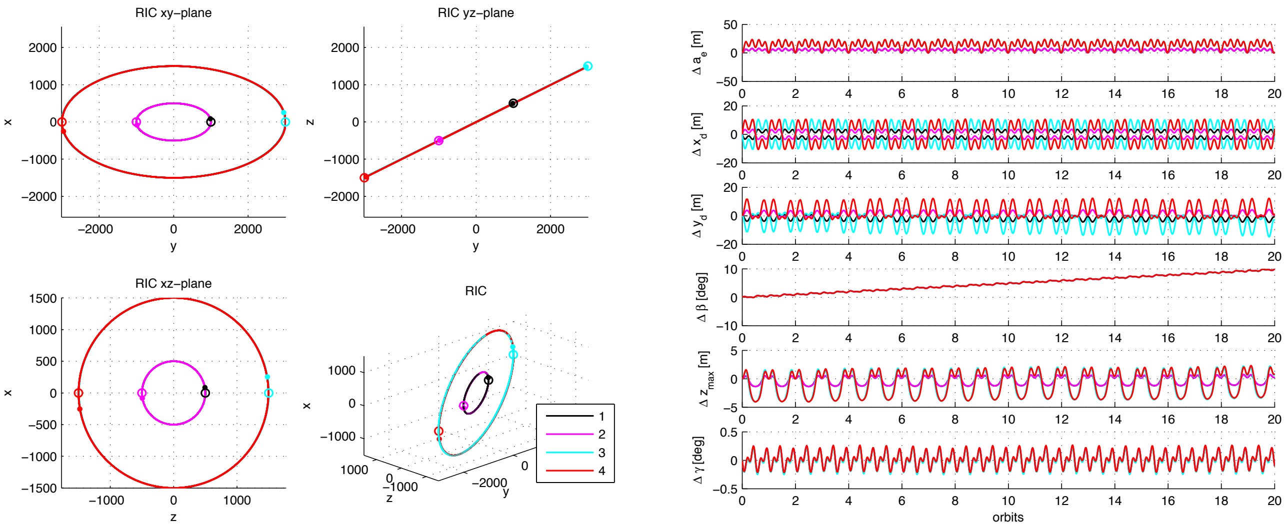

Figure 3: ROE secular drift in β for Nested cluster configuration with 4 modules, propagated for 20 orbits using a 20×20 gravity model. The orbit has an altitude of 600 km and is critically inclined at 63.43°.

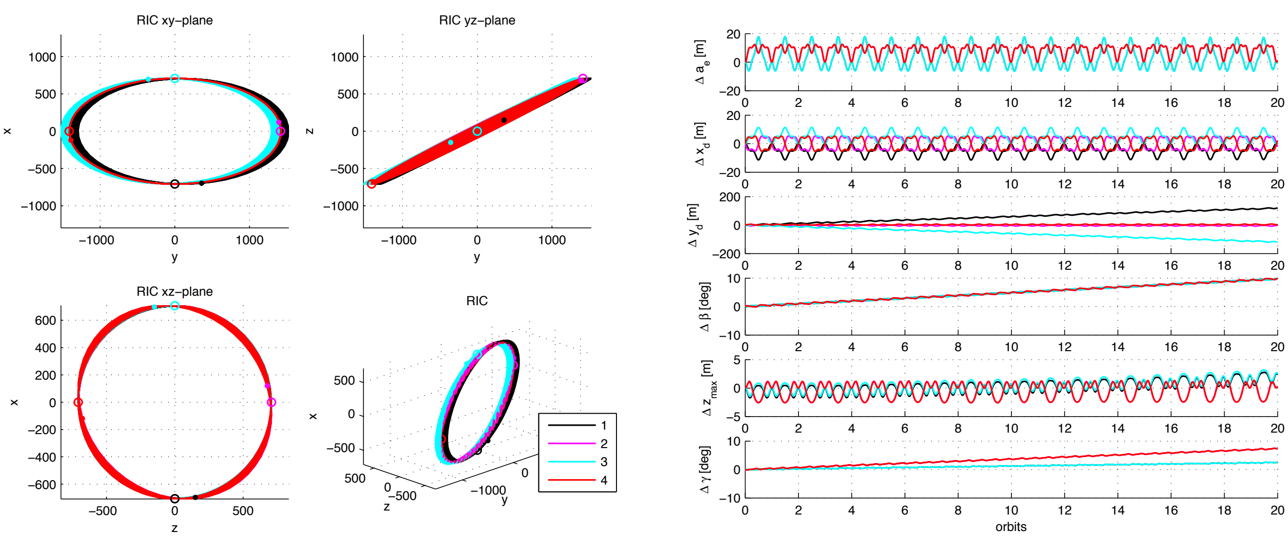

Figure 4: ROE secular drift in β, γ, and y_d for Circles-in-Circles cluster configuration with 4 modules, propagated for 20 orbits using a 20×20 gravity model. The orbit has an altitude of 600 km and is inclined at 45°.

Table 2: Relative Orbit Elements (ROE) for four module Circles-in-Circles formation in Fig. 4.

Module	a_e (m)	x_d (m)	y_d (m)	β (degrees)	z_{max} (m)	γ (degrees)
1	1414.2	0	0	0	707.1	0
2	1414.2	0	0	90	707.1	0
3	1414.2	0	0	180	707.1	0
4	1414.2	0	0	270	707.1	0

5. Packing Ratio

Clusters may maintain radio communications to share navigation, coordinate maneuvers, or distribute mission data. Communication systems are sensitive to distance, and are, along with fuel usage, a motivation to minimize the maximum distance between modules. The ratio of the maximum separation distance to the minimum separation distance is known as the packing ratio. Smaller packing ratios ratios allow for smaller cluster sizes while still maintaining minimum separation distances required by safety constraints. Additionally, as described in the section on passive safety, it is desirable to maintain a minimum separation distance in the radial-crosstrack plane. Therefore, the definition of packing ratio is modified to be the ratio of the maximum separation distance to the minimum separation distance in the radial-crosstrack plane.

$$r_p = \frac{d_{\max}}{d_{min-xz}} \tag{7}$$

By minimizing this ratio we are able to achieve the highest level of passive safety with the most compact cluster possible. The optimal solution to this problem is equivalent to the optimal packing problem detailed in [4], and can be simplified by attempting to find the smallest circle in which N congruent circles can fit inside. The solutions for two through seven modules are detailed in Fig. 5.

An optimal set of relative orbit elements based on these mathematical solutions is referred to as the Circles-in-Circles configuration. The four module solution was already shown in Fig. 4, and the seven module solution is shown in Fig. 6.

The Cross configuration, shown in Fig. 7, has a better packing ratio than the Nested configuration but shares its passive stability. The formation achieves a better packing ratio because, as is shown in Tab. 3, the modules with the largest semi-major axis, a_e, have the smallest crosstrack magnitudes, z_{max}. The Nested and Cross configurations are defined in the appendix and are shown for ten modules in Fig. 18. The packing densities of Nested, Cross, and Circles-in-Circles configurations are shown in Fig. 8.

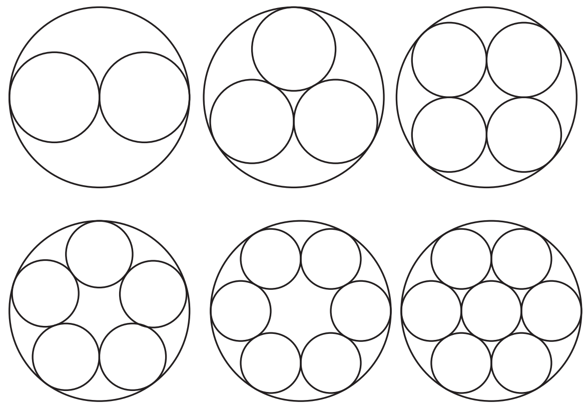

Figure 5: Optimal packing in the radial-crosstrack plane for two though seven modules.

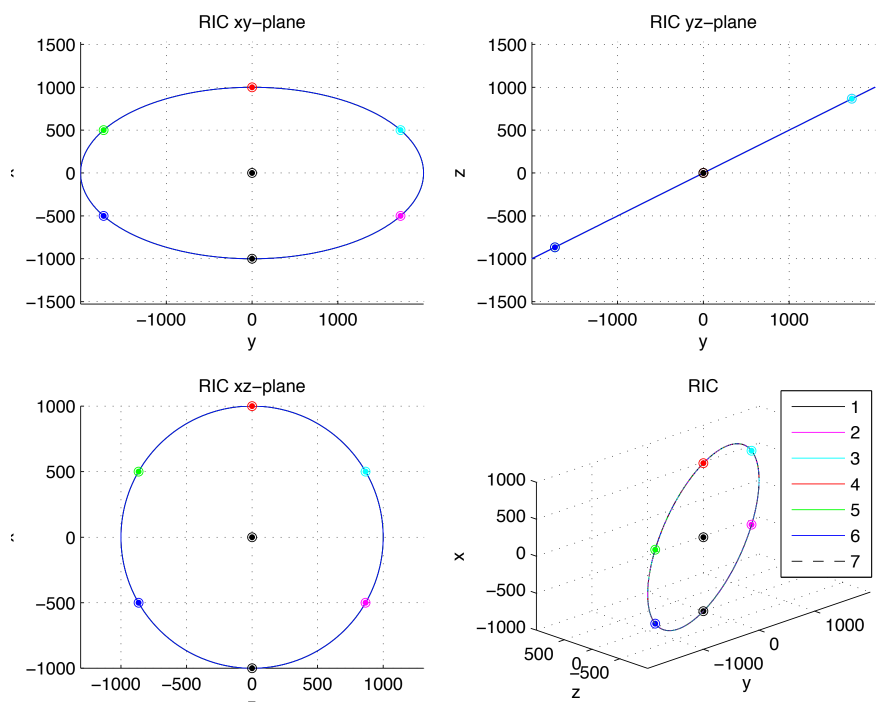

Figure 6: Optimal packing with Circles-in-Circles cluster configuration with 7 modules.

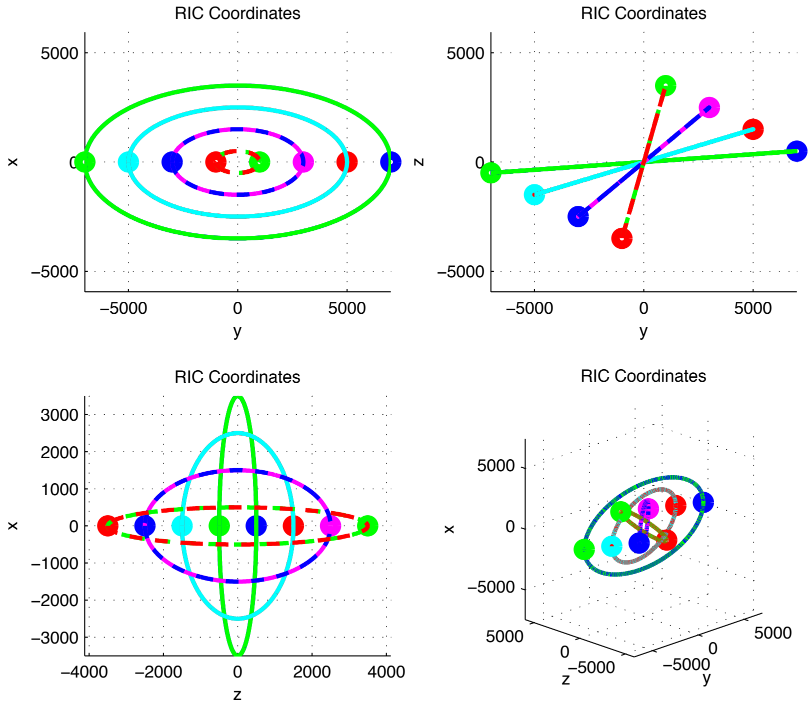

Figure 7: Cross cluster configuration with eight modules.

Table 3: Relative Orbit Elements (ROE) for eight module Cross formation in Fig. 7.

Module	a_e (m)	x_d (m)	y_d (m)	β (degrees)	z_{max} (m)	γ (degrees)
1	7000	0	0	90	500	0
2	7000	0	0	270	500	0
3	5000	0	0	90	1500	0
4	5000	0	0	270	1500	0
5	3000	0	0	90	2500	0
6	3000	0	0	270	2500	0
7	1000	0	0	90	3500	0
8	1000	0	0	270	3500	0

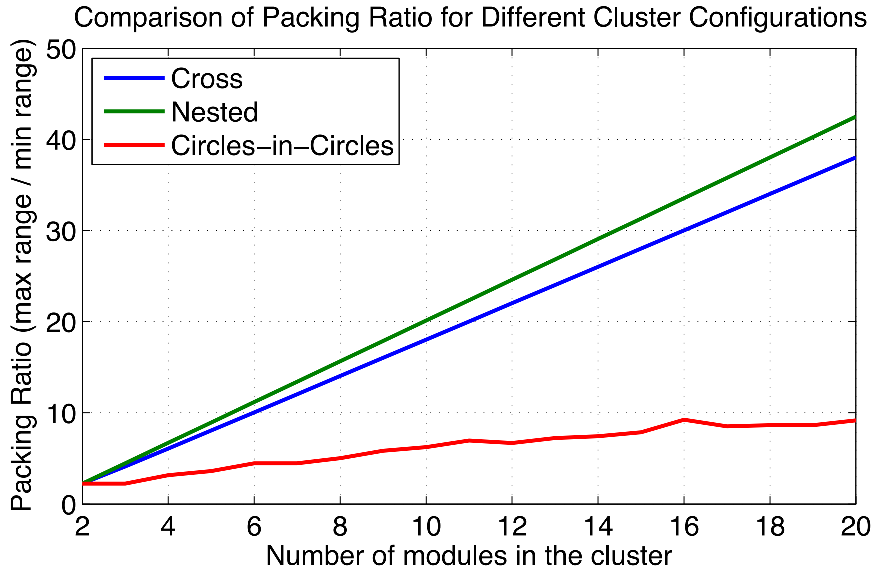

Figure 8: Comparison of packing ratio for various cluster configurations where smaller is better.

6. Cone Angle

Many communication systems utilize high bandwidth antennas that have tight pointing constraints. In order to minimize slewing, the inter-module cone angles should be taken into account in either the inertial or RIC frames. Additionally, any future missions utilizing power beaming between modules would benefit from a small maximum inter-module cone angle.

6.1. Cone Angle in the RIC Frame

The cluster configuration that minimizes cone angle in the RIC frame is String-of-Pearls, where the orbits only differ in y_d, however, this is undesirable for passive safety considerations. Nevertheless, two modules in passively safe ellipses that are offset in y_d, can achieve a small cone angle in the RIC frame. This concept can be extended by arranging the modules into two subclusters that are distributed along the v-bar. In this arrangement, each satellite can see two others in the other subcluster within a small cone angle. By passing data along the chain, any module can communicate with any other module in the cluster. Originally named by Jeremy Schwartz of Mittrio LLC, this Chopsticks formation allows many satellites to communicate with high gain antennas without requiring large slew maneuvers. A four module Chopsticks formation is shown in Fig. 9. The ROEs for the formation are shown in Tab. 4.

A graphical representation of the cone angles from module 1 and module 2 are shown in Fig. 10. Note that the cone angle to the modules in the other subcluster are very small, but the cone angles to modules in the same subcluster are a full 180°. For the safety ellipses shown in Fig. 9, the cone angles and the midpoints of the cone angles can be derived from the geometry with Eqs. 8 to 11 because the relative z_{max} is large enough that crosstrack motion determines the cone angle.

When designing clusters, one will often start with two sets of ROEs for two modules. Cone angles are easier to calculate for a single set of ROEs. This can be easily remedied by calculating the relative orbit elements of the second module with respect to the first by converting the ROEs into RIC coordinates using Eq. 4. Subtract the RIC coordinates and then convert back to relative orbit elements with Eq. 1. The resulting ROEs can then be used to calculate the cone angle and the offset between the ±v-bar of the RIC frame and midpoint of the cone angle:

$$\theta_1 = \arctan 2(z_{max}, \text{abs}(y_d) + a_e) \tag{8}$$

$$\theta_2 = \arctan 2(z_{max}, \text{abs}(y_d) - a_e) \tag{9}$$

$$\text{cone angle} = \theta_1 + \theta_2 \tag{10}$$

$$\text{midpoint offset} = \text{abs}(\theta_1 + \theta_2)/2 \tag{11}$$

Table 4: Relative Orbit Elements (ROE) for Four Module Chopsticks Formation in Fig. 9

Module	a_e (m)	x_d (m)	y_d (m)	β (degrees)	z_{max} (m)	γ (degrees)
1	1000	0	0	180	500	0
2	1000	0	6000	0	500	0
3	2000	0	6000	0	1000	0
4	2000	0	6000	180	1000	0

Table 5: Cone Angles between Modules in Fig. 9

Module	**1**	**2**	**3**	**4**
1		21.16°		9.796°
2	21.16°		9.796°	
3		9.796°		56.31°
4	9.796°		56.31°	

6.2. Cone Angle in the Inertial Frame

Cone angles in the inertial frame are less flexible. If the trajectory of the other module is entirely downrange or uprange, then the inertial cone angle will be a full 180°. If z_{max}, x_d, and y_d are set to zero and a_e is non-zero, then inertial cone angles with respect to the origin of $\sim 40°$ will be obtained. The inertial cone angles for such an arrangement are shown in Fig. 11. To ease interpretation of the figures, the inertial frame and the RIC frame were initially aligned. Also, note that the size of the cluster does not impact the cone angles. A passively safe geometry can be obtained if $z_{max} = \frac{a_e}{2}$. As seen in Fig. 12, this geometry will result in inertial cone angles of $\sim 60°$.

By packing four modules unevenly into a large ellipse, a pseudo-chopsticks formation can be created where each module can see two others on the other side of the ellipse. Figure 13 shows

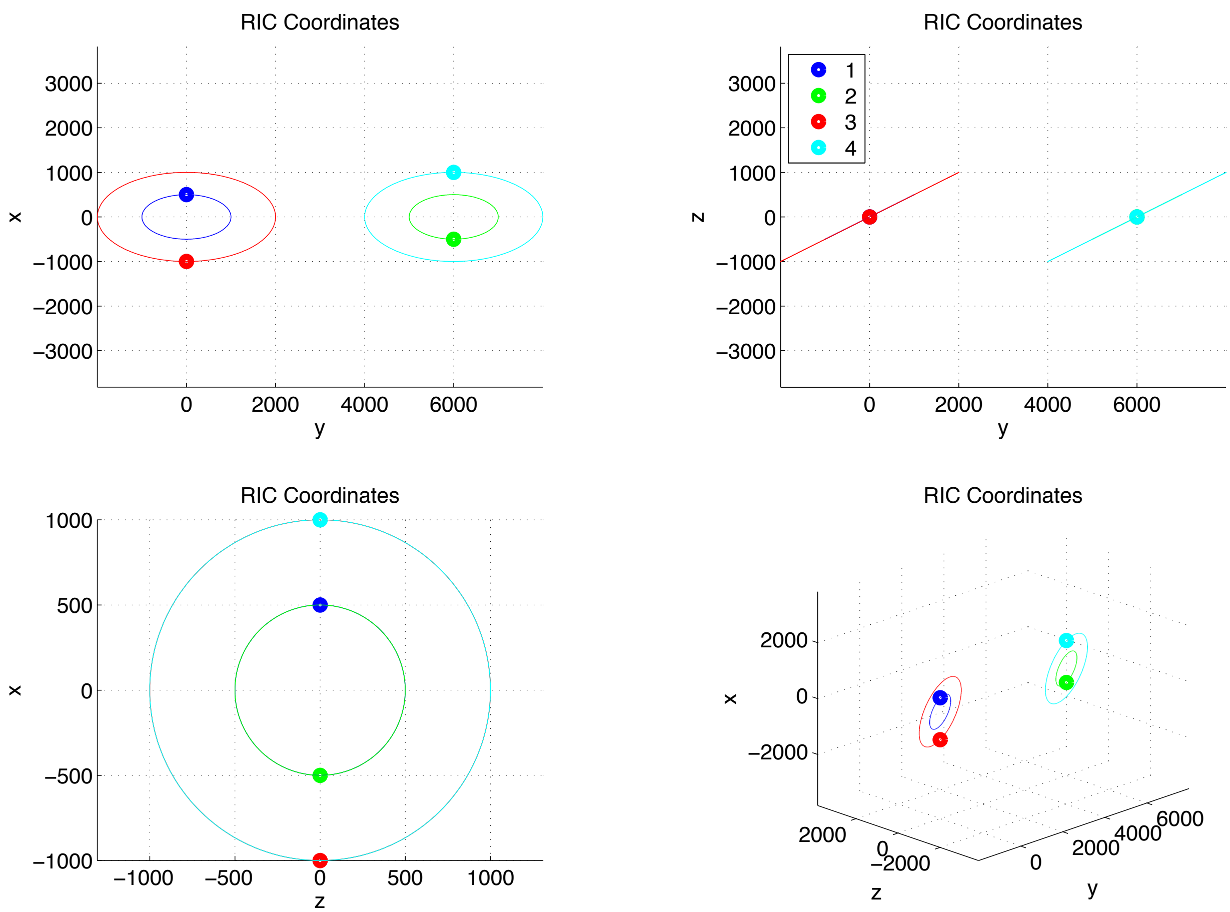

Figure 9: Four Module Chopstick Formation with Intrack Subcluster Seperation

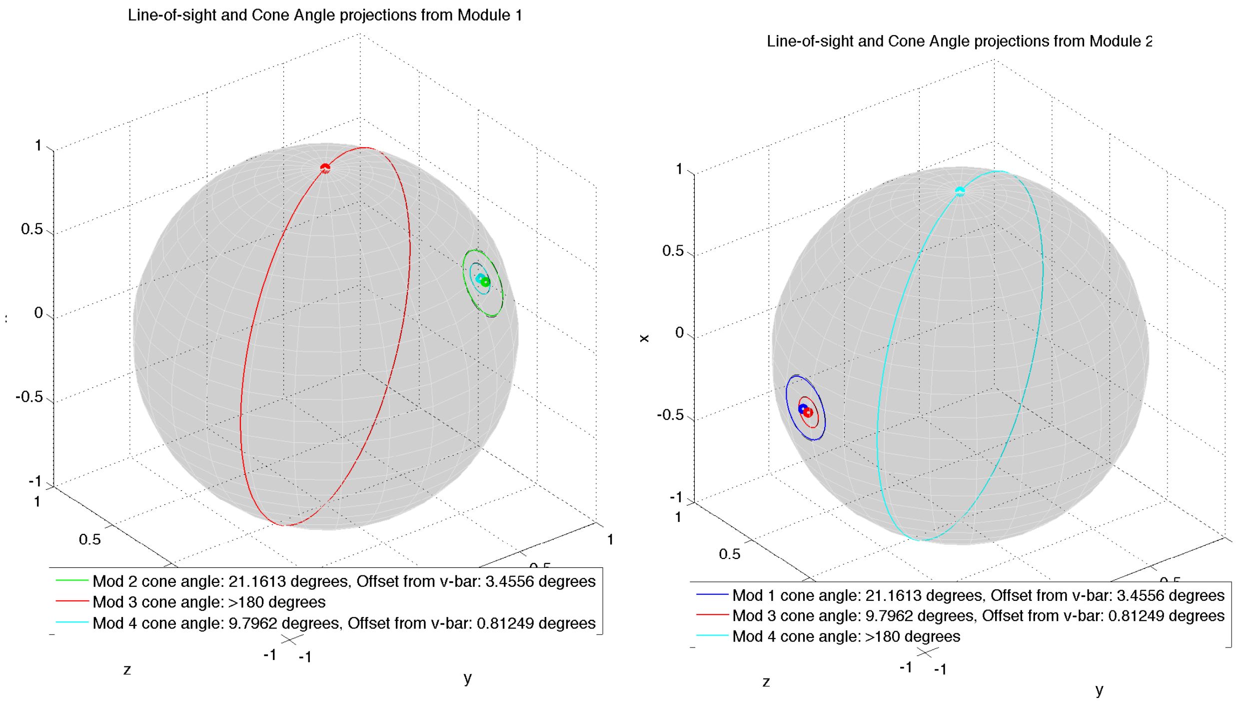

Figure 10: Projection of Line-of-Sight Angles and Resultant Cone Angles for Module 1 and Module 2 onto a Unit Sphere

four modules with a 30° β separation for the modules on opposite sides of an ellipse with $z_{max} = \frac{a_e}{2}$. The bottom right (green) module can enclose the two opposite modules with an inertial cone angle of $\sim 75°$.

7. Scalability

The ability to add more modules to an existing cluster in a uniform and systematic fashion should also be taken into account. Scalability can be viewed in two different ways. Static scalability allows a cluster configuration method that optimizes certain constraints to be adapted to different numbers of satellite modules. Dynamic scalability allows the cluster to add modules without significantly altering the configuration, minimizing fuel cost when ingressing a module into the cluster.

All of the configurations that have been discussed thus far have been designed with static scalability in mind. Each cluster type has configurations defined for 2 through 20 modules (as defined in the appendix). For more than 20 modules, the Circles-in-Circles (Fig. 18b) configuration would need more work. String-of-Pearls (Fig. 15), See-Saw (Fig. 16), Nested (Fig. 18a) and Cross (Fig. 18c) configurations can be expanded to an arbitrary number of modules.

Only some of the configurations scale dynamically. The Nested, String-of-Pearls, and See-Saw configurations dynamically scale with no reconfiguration required. For the Cross configuration a change in a_e and z_{max} is required to add modules to the cluster. Care must be taken to ensure the passive safety of the cluster while transitioning modules to their new relative orbits. For the Circles-in-Circles configuration adding modules to the cluster is even more problematic. It requires

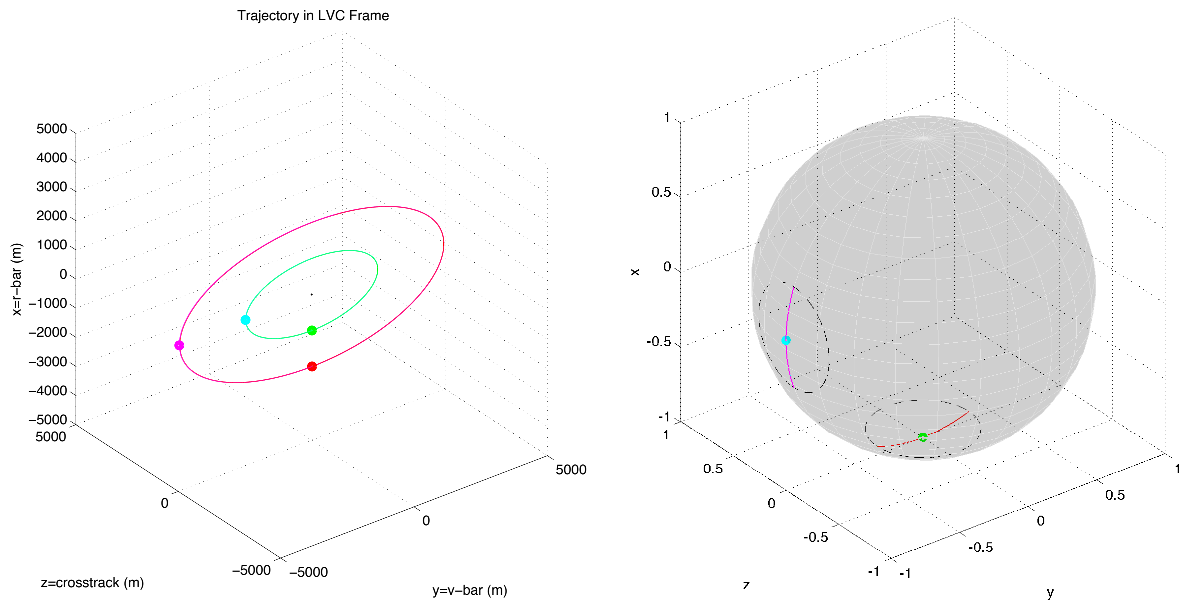

Figure 11: Inertial Cone Angles of $\sim 40^{\circ}$ with respect to the origin when z_{max}, x_d, and y_d are set to zero and a_e is non-zero

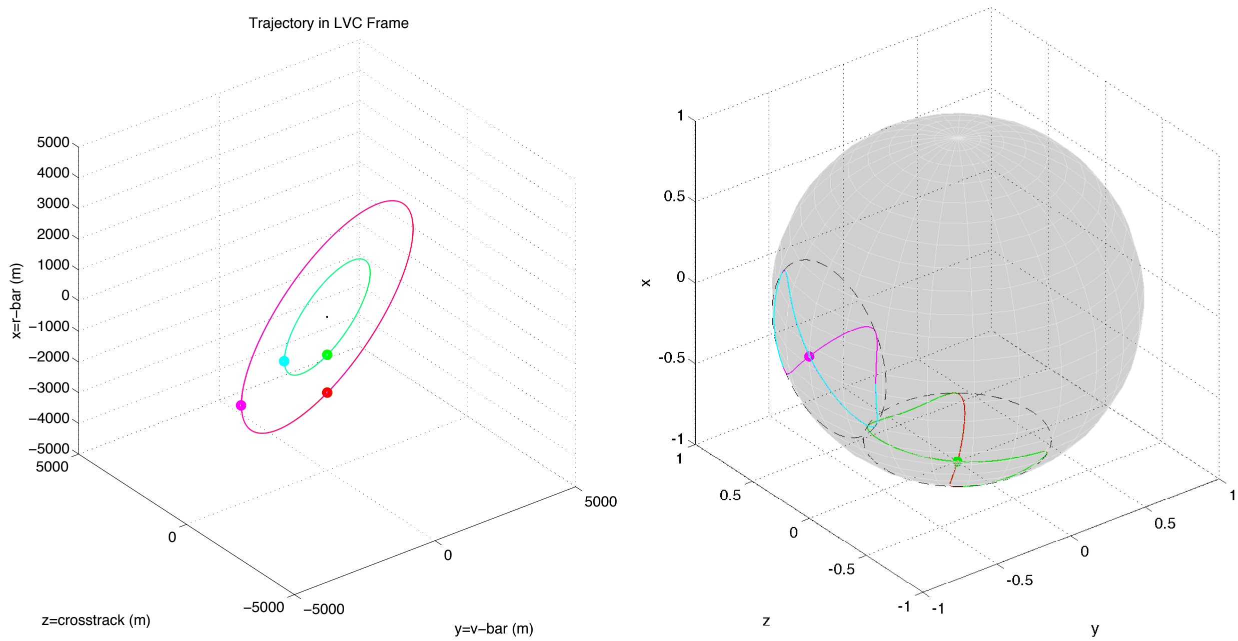

Figure 12: Inertial Cone Angles of $\sim 60^{\circ}$ with respect to the origin when x_d, and y_d are set to zero, a_e is non-zero, and $z_{max} = \frac{a_e}{2}$

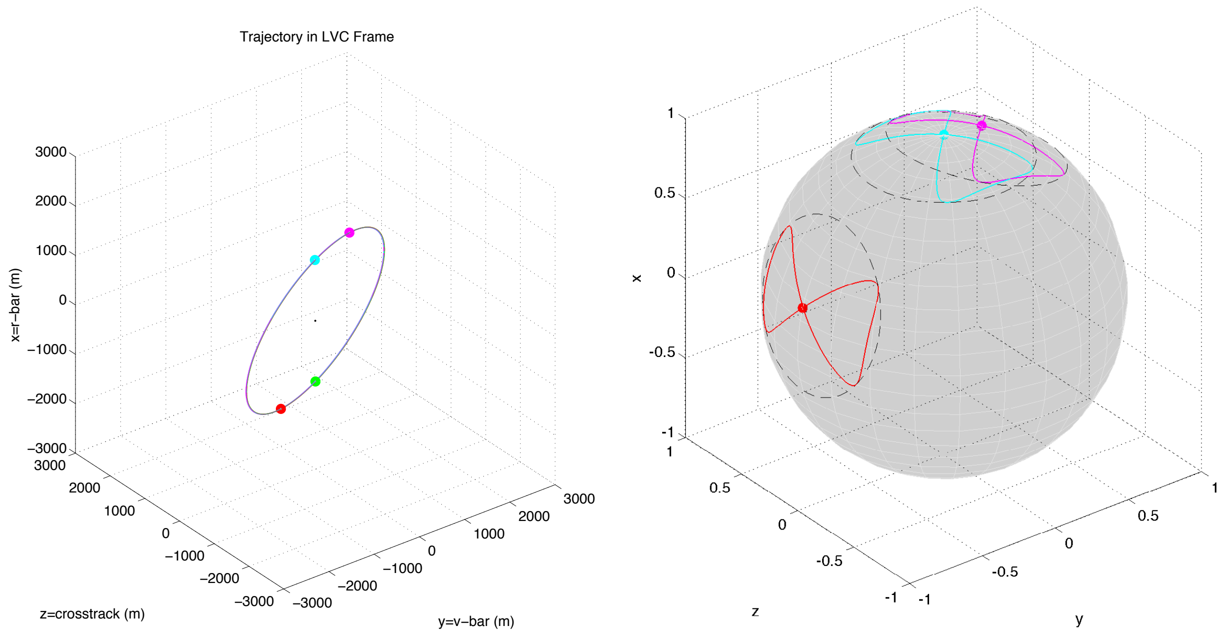

Figure 13: Inertial Cone Angles of $\sim 75^\circ$ to the two modules opposite the bottom-right module (green) in a pseudochopsticks formation with $z_{max} = \frac{a_e}{2}$.

adjusting not only a_e and z_{max}, but also the in-plane phase angle β of the modules which is more costly in terms of fuel.

One simple way to avoid having to adjust the relative orbits of the existing modules in a cluster to make room for new modules, is to design the cluster with empty spots to begin with.

8. Observability

Inter-satellite measurements provide only relative state information to the filter and must be augmented by some absolute measurements. However, relative measurements can improve the relative state knowledge by orders of magnitude over simple differencing of absolute states. Highly accurate relative state knowledge can improve the performance of guidance and control algorithms with the net result of lowering the probability of collision and reducing fuel consumption. Relative measurements include relative angle, range, and range-rate measurements, which can be realized through several sensors such as Light Detection and Ranging (LIDAR), radar, and some wireless communication systems. If range and angle information is combined, then the total relative state can be observed. If only one or the other is available, observability is more difficult. As seen in Fig. 11, relative satellite motion at close ranges has the curious characteristic of identical line-of-sight tracks irrespective of range. This can only be overcome if forced motion is introduced into the problem [11], or if the ranges are large enough that curvature of the orbit can be observed [12].

Range and range-rate measurements are more useful than angle measurements in these situations. Relative orbit motion generally precludes having three orthonormal measurements available at all times, and relative state observability for two modules with only range measurements is dubious, with convergence possibly requiring several orbits [3]. Careful construction of the cluster geometry for four modules can provide reliable observability over a single orbit.

In the following figures, the relative range observability characteristics of some representative four module cluster geometries are analyzed. This analysis was performed by processing relative range measurements in a navigation filter and analyzing the evolution of the state covariance. The filter is given perfect initial conditions and the processed measurements are perfect (though the filter processes them as if they had errors). The result is a basic linear covariance analysis that captures the nature of the observability problem. If the covariance is bounded over the simulated interval, then the problem is considered observable. The degree of observability was not analyzed so the specific values for filter process noise, measurement noise, etc. are not important.

The geometries chosen represent basic cluster types that can be constructed for stable clusters and are shown in the RIC frame. They give a good overview of the problem without looking at every possible geometry. There are relative range measurements between each module (for a total of six measurements for a cluster of four modules). Though not shown here, range rate measurements have the same observability characteristics as range measurements.

The most easily understood case is for a planar ellipse with four satellites as shown in Fig. 14a. For the planer case, if each module ranges to every other module, there is no observability of the state in the out-of-plane direction. Thus, as seen in Fig. 14b, the covariance of the cyan satellite's crosstrack position grows without bound. Even if z_{max} is made non-zero, the cluster will remain unobservable perpendicular to the plane of the ellipse.

The String-of-Pearls configuration (Fig. 15a) places all of the spacecraft on the reference orbit, but at different locations on that orbit. This would correspond to ROEs all equal to zero except for y_d. The geometry is not observable with range measurements (Fig. 15b). However, adding out-of-phase crosstrack motion to the String-of-Pearls configuration (to generate a See-Saw configuration as seen in Fig. 16a) will allow observability using range measurements (Fig. 16b). The See-Saw configuration corresponds to non-zero z_{max} with different ψ angles for each module.

A stacked ellipse configuration as seen in Fig. 17a can be built by setting $z_{max} = \frac{a_e}{2}$ where a_e is non-zero, $\gamma = x_d = 0$, and each module is given a different y_d and β. If all members were in phase (same β), this case would degenerate into a String-of-Pearls formation. When range measurements are processed in a filter, the relative state is observable (Fig. 17b).

It can be concluded that relative trajectories that are not colinear when projected into the intrack-crosstrack plane over the course of an orbit are observable with range measurements. Radial offset (non-zero x_d) causes intrack drift, so observing intrack relative position can observe radial position.

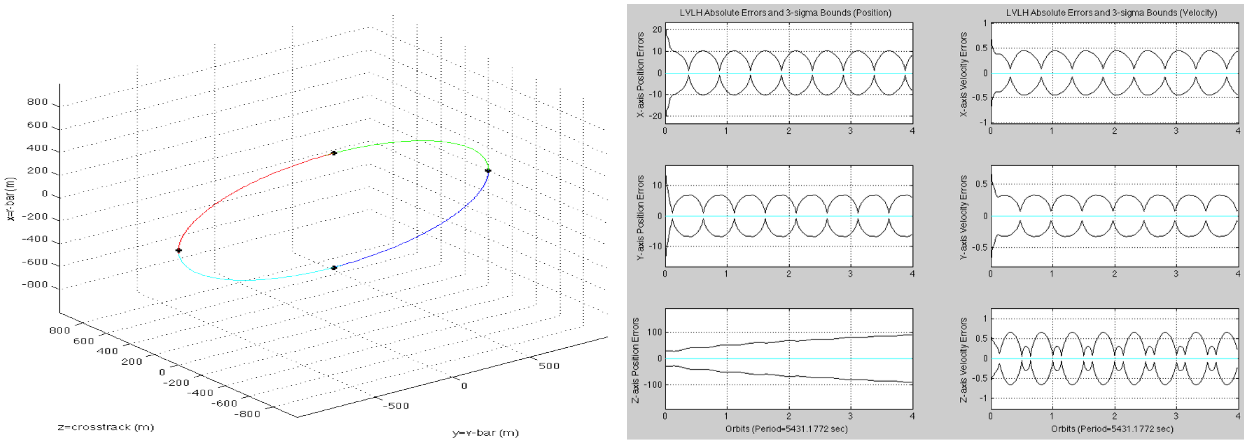

(a) Planar Cluster Configuration

(b) Covariance Analysis of Relative Range Observability of Planer Case

Figure 14: Planar Cluster Configuration Observability

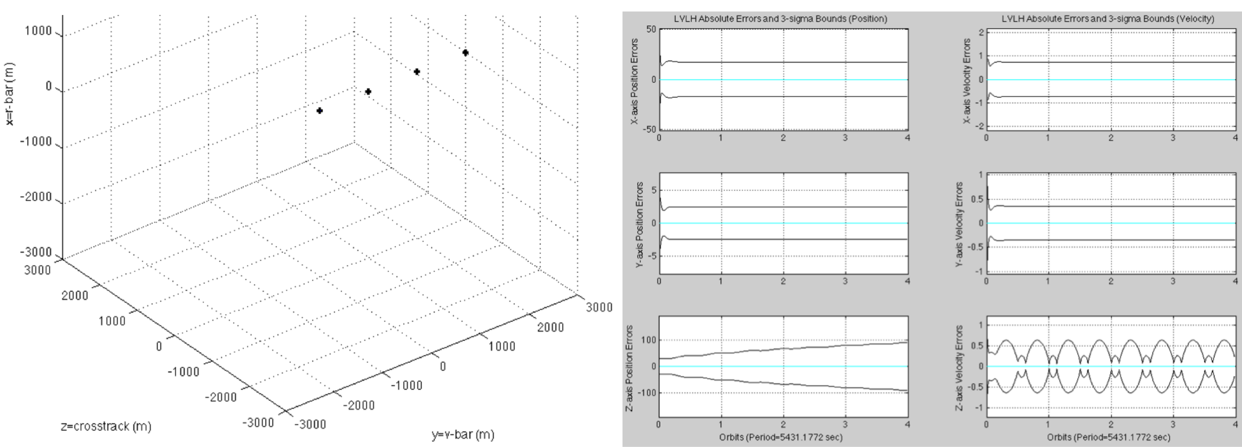

(a) String-of-Pearls Cluster Configuration

(b) Covariance Analysis of Relative Range Observability of String-of-Pearls Cluster Configuration

Figure 15: String-of-Pearls Cluster Configuration Observability

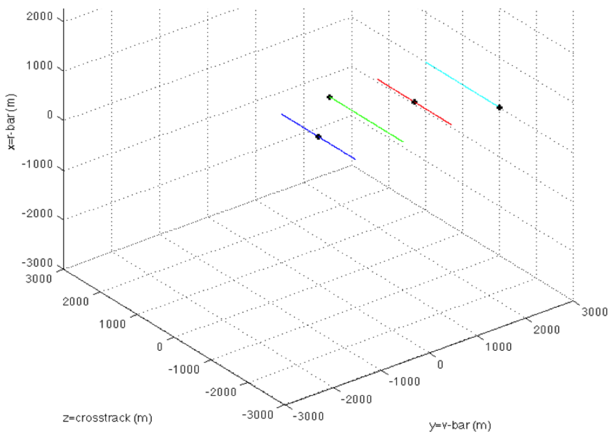

(a) See-Saw Cluster Configuration

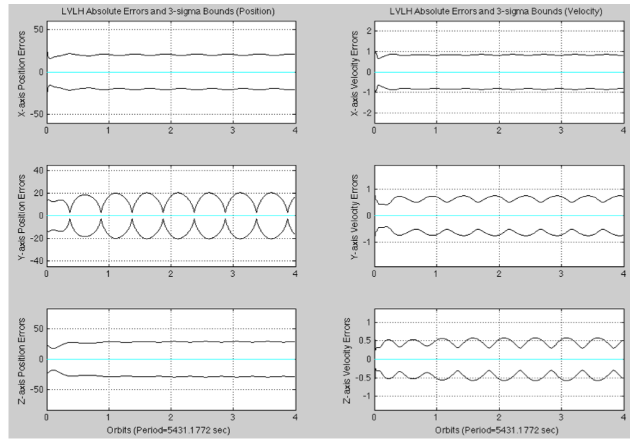

(b) Covariance Analysis of Relative Range Observability of See-Saw Cluster Configuration

Figure 16: See-Saw Cluster Configuration Observability

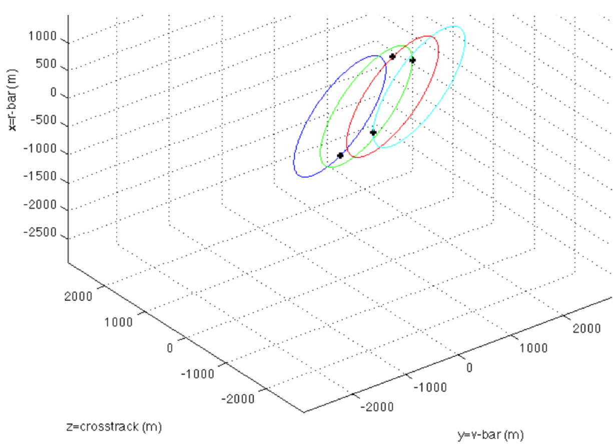

(a) Stacked Cluster Configuration

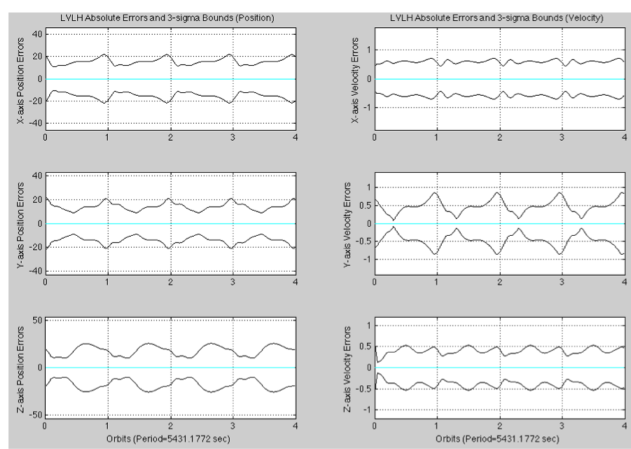

(b) Covariance Analysis of Relative Range Observability of Stacked Cluster Configuration

Figure 17: Stacked Cluster Configuration Observability

9. Example Passively Safe Clusters

A few passively safe cluster configurations that optimally satisfy some of these constraints are Circles-in-Circles, Nested, and Cross. The strengths and weaknesses of the different configurations are shown in Tabs. 6 to 8. Ten module clusters in Circles-in-Circles, Nested, and Cross configurations that maintain a 1 km minimum separation distance are shown in Fig. 18. Overall, the Nested configuration has the best balance among the metrics. It is stable, scalable, and, when broken into two subclusters, observable. Two subclusters of the Nested configuration can have small cone angles with the Chopsticks approach. The Cross configurations sacrifice scalability and the possibility of small cone angles in order to achieve a slightly better packing ratio. This is an poor sacrifice for many applications. The Circles-in-Circles configurations are not as stable or scalable as the Nested configuration, but are significantly more compact. If atmospheric drag is the primary destabilizing force, or omnidirectional antennas are used, it may be a superior configuration.

Table 6: Summary of Nested strengths and weaknesses

Metric	Comments about Nested Configuration
Passive Safety	Passively safe
Stability	The modules can be placed at the same inclination, thus the configuration is stable to gravitational effects, but less stable to differential atmospheric drag effects in comparison to Circles-in-Circles because of a poor packing ratio
Packing Ratio	Packing ratio is poor (Fig. 8)
Cone Angle	If broken into two subclusters (with y_d separation), then small cone angles can be obtained using Chopsticks approach
Scalability	Very scalable. New modules can be added to the cluster without requiring the resident modules to be reconfigured
Observability	Because the configuration is collinear in the intrack-crosstrack plane, it must be broken into subclusters to have observability with range or range-rate measurements

Table 7: Summary of Circles-in-Circles strengths and weaknesses

Metric	Comments about Circles-in-Circles Configuration
Passive Safety	Passively safe
Stability	The modules are not at the same inclination, thus the configuration is not very stable to gravitational effects, but more stable to differential atmospheric drag effects because of a good packing ratio
Packing Ratio	Optimal packing ratio while maintaining passive safety (Fig. 8)
Cone Angle	If broken into two subclusters (with y_d separation), then small cone angles can be obtained using chopsticks approach
Scalability	Optimal solutions for up to 20 modules are known, but significant reconfiguration is required to accommodate other modules joining the cluster
Observability	Because the configuration is collinear in the intrack-crosstrack plane, it must be broken into subclusters to have observability with range or range-rate measurements

Table 8: Summary of Cross strengths and weaknesses

Metric	Comments about Cross Configuration
Passive Safety	Passively safe
Stability	The modules can be placed at the same inclination, thus the configuration is stable to gravitational effects, but less stable to differential atmospheric drag effects in comparison to Circles-in-Circles because of a poor packing ratio.
Packing Ratio	Packing ratio is poor, but slightly better than the Nested configuration (Fig. 8)
Cone Angle	Cone angles are poor, even if broken into two subclusters (with y_d separation), the max intermodule cone angles will be fairly large.
Scalability	Significant reconfiguration is required to accommodate other modules joining the cluster
Observability	Marginally observable without subclusters, but if the initial conditions are poor, relative range and range-rate measurements can converge to the wrong solution. Subclusters will improved observability.

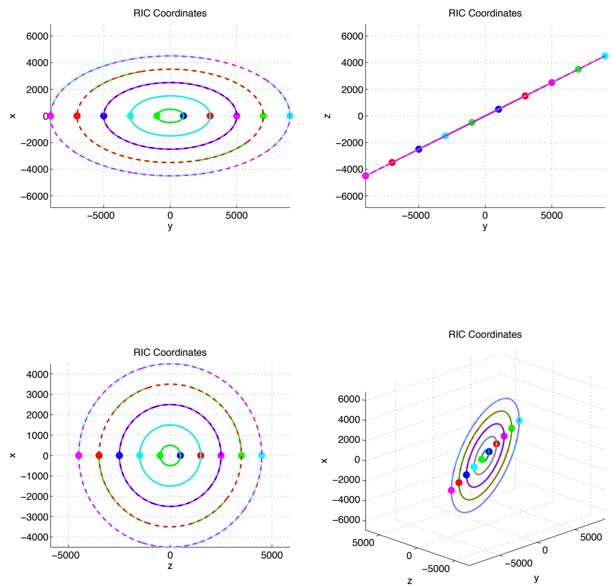

(a) Nested Configuration

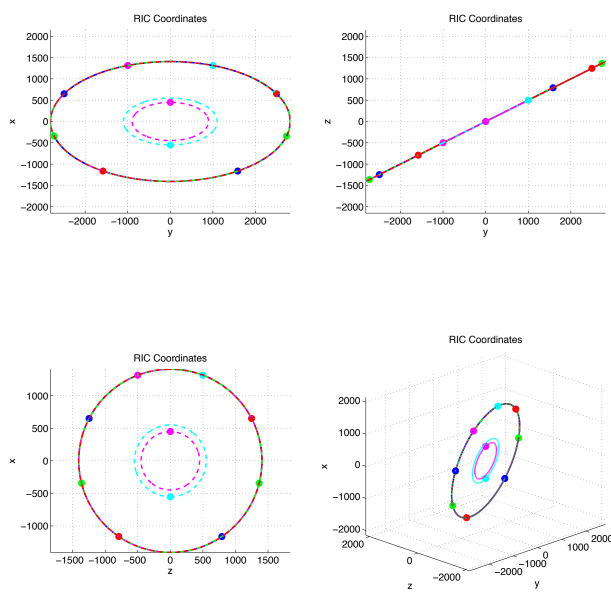

(b) Circles-in-Circles Configuration

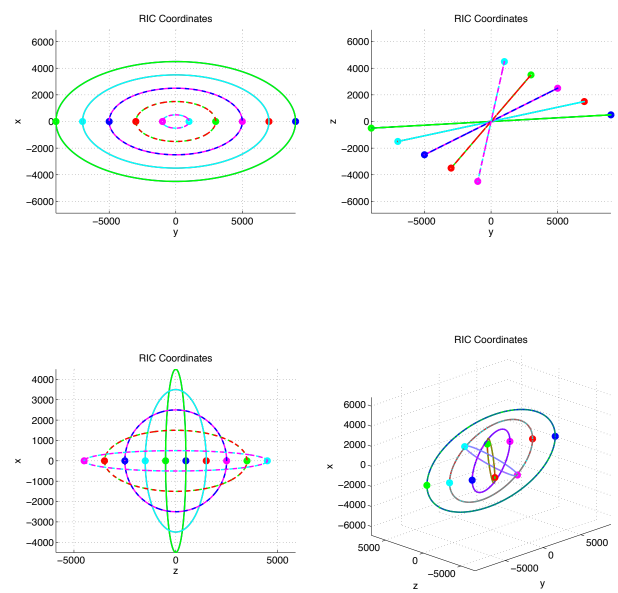

(c) Cross Configuration

Figure 18: Nested, Circles-in-Circles and Cross cluster configurations (shown in meters) for 10 modules.

10. Acknowledgment

We are grateful for the contributions of all the members of the Emergent Space Technologies System F6 Team.

This work was sponsored by DARPA under the System F6 program. The views expressed are those of the authors and do not reflect the official policy or position of the Department of Defense or the U.S. Government.

11. References

[1] Vallado, D. A. and McClain, W. D., *Fundamentals of Astrodynamics and Applications*, The Space Technology Library, Microcosm Press, Hawthorne, CA, 3rd ed., 2007.

[2] Brown, O., Eremenko, P., and Bille, M., "Fractionated Space Architectures: Tracing the Path to Reality," *Small Satellite Conference*, Logan, Utah, 2009.

[3] Maessen, D. C. and Gill, E., "Relative Orbital Element Estimation and Observability Analysis for Formation Flying Satellites using Inter-Satellite Range Measurements Only," *AIAA Guidance, Navigation, and Control Conference*, Toronto, Canada, August 2-5, 2010 2010.

[4] Graham, R. L., Lubachevsky, D., Nurmela, K. J., and Ostergglrd, P. R. J., "Dense Packings of Congruent Circles in a Circle," *Discrete Mathematics*, Vol. 181, 1998, pp. 139–154.

[5] Fodor, F., "The Densest Packing of 13 Congruent Circles in a Circle," *Contributions to Algebra and Geometry*, Vol. 44, No. 2, 2003, pp. 431–440.

[6] Fodor, F., "The Densest Packing of The Densest Packing of 12 Congruent Circles in a Circle," *Contributions to Algebra and Geometry*, Vol. 41, No. 2, 2000, pp. 401–409.

[7] Goldberg, M., "Packing of 14, 16, 17 and 20 Circles in a Circle," *Mathematics Magazine*, Vol. 44, No. 3, May 1971, pp. 134–139.

[8] D'Amica, S., Ardaens, J.-S., and Larsson, R., "Spaceborne Autonomous Formation Flying Experiment on the PRISMA Mission," *Journal of Guidance, Control, and Dynamics*, Vol. 35, No. 3, 2012.

[9] Gaylor, D. E. and Barbee, B. W., "Algorithms for Safe Spacecraft Proximity Operations," *AAS/AIAA Spaceflight Mechanics Meeting*, 2007.

[10] Alfriend, K. T., Vadali, S. R., Gurfil, P., How, J. P., and Breger, L. S., *Spacecraft Formation Flying: Dynamics, Control and Navigation*, Elsevier, Kidlington, Oxford, UK, 1st ed., 2010.

[11] Schmidt, J., *Analysis of Square-root Kalman Filters for Angles-only Orbital Navigation and the Effects of Sensor Accuracy on State Observability*, Master's thesis, Utah State University, Logan, Utah, 2010.

[12] Bingham, B. E. and Geller, D. K., *Preliminary Orbit Determination for Orbital Rendezvous using Gauss' Method*, Master's thesis, Utah State University, Logan, Utah, 2007.

[13] Alfriend, K. T., Schaub, H., and Gim, D.-W., "Gravitational Perturbations, Nonlinearity and Circular Orbit Assumption Effects on Formation Flying Control Strategies," *Advances in the Astronautical Sciences*, Vol. 104, No. AAS 00-012, 2000, pp. 139–158.

[14] Gustafson, D. E. and Kriegsman, B. A., "A Guidance and Navigation System for Automatic Stationkeeping in Earth Orbit," *Journal of Spacecraft and Rockets*, Vol. 10, No. 6, June 1973, pp. 369–376.

[15] Lovell, T. A. and Tollefson, M. V., "Calculation of Impulsive Hovering Trajectories via Relative Orbit Elements," *AIAA/AAS Astrodynamics Specialist Conference and Exhibit*, No. AAS 05-409, American Astronamical Society, San Diego, CA 92198, August 2005.

[16] Lovell, T. A. and Tragesser, S. G., "Guidance for Relative Motion of Low Earth Orbit Spacecraft Based on Relative Orbit Elements," *AIAA/AAS Astrodynamics Specialist Conference and Exhibit*, No. AIAA-2004-4988, American Institute of Aeronautics and Astronautics, Providence, RI, August 2004.

[17] Vadali, S. R., Sengupta, P., Yan, H., and Alfriend, K. T., "Fundamental Frequencies of Satellite Relative Motion and Control of Formations," *Journal of Guidance, Control, and Dynamics*, Vol. 31, No. 5, September-October 2008.

[18] Sabatini, M., Izzo, D., and Palmerini, G. B., "Invariant Relative Satellite Motion," *ACT workshop on Innovation Concepts*, ESA-ESTEC, January 2008.

Appendix: Cluster Definitions

For all cluster geometries the following relative orbit elements are defined the same

$$\begin{aligned} \gamma &= 0 \\ x_d &= 0 \\ y_d &= 0 \end{aligned}$$

N is the total number of modules in the cluster, n represents the nth module, and d_{min} is the minimum intermodule distance.

Nested

Examples of the Nested configuration are shown in Figs. 2, 3, and 18. The ROEs for a Nested configuration can be populated for N modules with the following algorithm:

$$
\begin{aligned}
a_e &= \begin{cases} nd_{min} & \text{if } n \text{ is odd,} \\ (n-1)\, d_{min} & \text{otherwise.} \end{cases} \\
z_{max} &= \frac{a_e}{2} \\
\beta &= \begin{cases} 90^\circ & \text{if } n \text{ is odd,} \\ 270^\circ & \text{otherwise.} \end{cases}
\end{aligned}
$$

These β values should correspond to the ascending or descending node of the orbit in order to build a configuration where all the modules are at the same inclination.

Circles-in-Circles

Examples of the Circles-in-Circles configuration are shown in Figs. 6 and 18. For any number of modules in the cluster the crosstrack amplitude is defined as $z_{max} = \frac{a_e}{2}$. The equations used to obtain a_e and β are dependent upon the number of modules in the cluster. Equations derived using [7, 4, 6, 5] are given in Tab. 9 for clusters with 2 to 20 modules.

Cross

Example of the Cross configuration are shown in Figs. 7 and 18. The ROEs for a Cross configuration can be populated for N modules with the following algorithm:

$$
\begin{aligned}
a_e &= 2d_{min}\, \text{floor}\left(\frac{n+1}{2}\right) - 1 \\
z_{max} &= d_{min}\, \text{floor}\left(\frac{N-n+2}{2}\right) - 0.5 \\
\beta &= \begin{cases} 90^\circ & \text{if } n \text{ is odd,} \\ 270^\circ & \text{otherwise.} \end{cases}
\end{aligned}
$$

These β values should correspond to the ascending or descending node of the orbit in order to build a configuration where all the modules are at the same inclination.

Table 9: Semi-major axis, a_e, and in plane phase angle, β, for Circles-in-Circles in terms of d_{min}

number of modules	a_e	β (deg)
2-6	$d_{min}\csc\frac{\pi}{N}$	$\frac{360^\circ}{N}(n-1)$
7-9	$\begin{cases} d_{min}\csc\frac{\pi}{N} & \text{if } n<N, \\ 0 & \text{if } n=N. \end{cases}$	$\frac{360^\circ}{N-1}(n-1)$
10	$\begin{cases} 2.813\,d_{min} & \text{if } n<9, \\ 0.964\,d_{min} & \text{if } n=9, \\ 1.036\,d_{min} & \text{if } n=10. \end{cases}$	$\begin{cases} 41.647^\circ n-7.411^\circ & \text{if } n<9, \\ 0^\circ & \text{if } n=9, \\ 180^\circ & \text{if } n=10. \end{cases}$
11	$\begin{cases} d_{min}\csc\frac{\pi}{9} & \text{if } n<10, \\ d_{min}\left(\csc\frac{\pi}{9}-\sqrt{3}\right) & \text{otherwise.} \end{cases}$	$\begin{cases} 40^\circ(n-1) & \text{if } n<10, \\ 100^\circ & \text{if } n=10, \\ 260^\circ & \text{if } n=11. \end{cases}$
12	$\begin{cases} 3.03\,d_{min} & \text{if } n<10, \\ d_{min}\csc\frac{\pi}{3} & \text{otherwise.} \end{cases}$	$\begin{cases} 120^\circ(n-1)-38.55^\circ & n=1,2,3, \\ 120^\circ(n-4) & n=4,5,6, \\ 120^\circ(n-7)+38.55^\circ & n=7,8,9, \\ 120^\circ(n-10) & n=10,11,12. \end{cases}$
13	$\begin{cases} d_{min}\csc\frac{\pi}{10} & \text{if } n<11, \\ d_{min}\csc\frac{\pi}{3} & \text{otherwise.} \end{cases}$	$\begin{cases} 36^\circ(n-1) & \text{if } n<11, \\ 120^\circ(n-11) & \text{otherwise.} \end{cases}$
14	$\begin{cases} 3.328\,d_{min} & \text{if } n<11, \\ 1.443\,d_{min} & \text{if } n=11, \\ 1.536\,d_{min} & \text{if } n=12, \\ 1.336\,d_{min} & \text{otherwise.} \end{cases}$	292.643, 327.611, 2.579, 37.548, 72.516, 107.484, 142.452, 177.421, 212.389, 247.357, 90, 270, 357.99, 182.01
15	$\begin{cases} d_{min}\sqrt{\left(\cot\frac{\pi}{5}+2\right)^2+1} & \text{if } n<11, \\ d_{min}\csc\frac{\pi}{5} & \text{otherwise.} \end{cases}$	$\begin{cases} 72^\circ\left(n-\frac{1}{2}\right)+16.5^\circ & \text{if } n<6, \\ 72^\circ(n-5.5)-16.5^\circ & \text{if } 6\le n<11, \\ 72^\circ(n-11) & \text{otherwise.} \end{cases}$
16	$\begin{cases} 3.615\,d_{min} & \text{if } n<12, \\ 1.812\,d_{min} & \text{if } n=12, \\ 1.63\,d_{min} & \text{if } n=13,15, \\ 1.72\,d_{min} & \text{if } n=14,16. \end{cases}$	289.431, 321.544, 353.658, 25.772, 57.886, 90, 122.114, 154.228, 186.342, 218.456, 250.569, 270, 52.162, 338.922, 127.838, 211.078
17	$\begin{cases} 3.809\,d_{min} & \text{if } n<8, \\ 1.943\,d_{min} & \text{if } n=8,9, \\ 0.081\,d_{min} & \text{if } n=10, \\ 2.026\,d_{min} & \text{if } n=11,12, \\ 2.081\,d_{min} & \text{if } n=13, \\ 3.809\,d_{min} & \text{otherwise.} \end{cases}$	358.6640, 29.11, 59.555, 90, 120.445, 150.89, 181.336, 44.332, 135.668, 270, 339.86, 200.14, 270, 321.056, 218.944, 290.611, 249.389
18-19	$\begin{cases} d_{min}\csc\frac{\pi}{12} & \text{if } n<13, \\ d_{min}\csc\frac{\pi}{6} & \text{if } 13\le n<19, \\ 0 & \text{otherwise.} \end{cases}$	$\begin{cases} 30^\circ\left(n-\frac{1}{2}\right) & \text{if } n<13, \\ 60^\circ(n-13) & \text{if } 13\le n<19, \\ 0^\circ & \text{otherwise.} \end{cases}$
20	$\begin{cases} 4.122\,d_{min} & \text{if } n<13, \\ 2.235\,d_{min} & \text{if } n=13,17, \\ 2.805\,d_{min} & \text{if } n=14, \\ 2.193\,d_{min} & \text{if } n=15,18, \\ 2.172\,d_{min} & \text{if } n=16,19, \\ 0 & \text{if } n=20. \end{cases}$	295.571, 323.649, 351.727, 19.805, 47.883, 75.961, 104.039, 132.117, 160.195, 188.273, 216.351, 244.429, 63.426, 270, 9.74, 315.198, 116.574, 170.26, 224.802, −90